This article has been accepted for publication in a future issue of this journal, but has not been fully edited. Content may change prior to final publication. Citation information: DOI 10.1109/TEC.2019.2930819, IEEE Transactions on Energy Conversion

Performance Analysis of Medium Voltage Grid Integration of PV Plant Using Modular Multilevel Converter

Anirudh Budnar Acharya, Mattia Ricco, *Member, IEEE,* Dezso Sera, *Senior Member, IEEE,* Remus Teoderscu, *Fellow, IEEE,* Lars E Norum, *Member, IEEE,*

***Abstract*—Modular Multilevel Converter (MMC) topology has emerged as an attractive solution for Photovoltaic (PV) applications. Such a structure due to its inherent modularity allows distributed architecture of utility scale PV plant. Moreover, converters scalability allows for direct connection to the medium voltage grid by avoiding the need for the step-up transformer. The isolation is provided at the interface between the PV array and the MMC by using an isolated DC-DC converter. In this work the MMC performance is evaluated and compared with the main central inverter configurations in terms of annual energy yield, efficiency and levelized cost of energy. Efficiency curve from no load to full load is obtained for the MMC through simulations using standard IGBT half-bridge modules. It is seen that the efficiency curve is flat for a wide range of loads resulting in a higher annual energy yield and lower Levelized Cost of Energy (LCOE).**

***Index Terms*—Modular Multilevel Converter, Utility Scale PV Plant, Medium Voltage, Annual Energy Yield, Central Inverter, Levelized Cost of Energy.**

I. Introduction

PHOTOVOLTAIC (PV) plants at utility scale normally employ the single stage two-level (2L) or three-level (3L) inverters as state-of-the-art Central Inverter (CI). The line side step-up transformer facilitates the connection to Medium Voltage (MV) AC grid. Several such CI units are connected in parallel to meet the desired power level [1]. The CI is a DC-AC converter, the PV array is connected to the common DC link. The DC link voltage is allowed to vary over certain range in order to track the Maximum Power Point Tracking (MPPT) of the PV array. The maximum efficiency of the CI is based on the choice of both the converter topology and switching devices and varies between 95-98%. The main advantages of CI are low cost and reduced complexity in terms of converter topology, control and communication. However, the CI is highly susceptible to partial shading, soiling, panel mismatch and defects in the PV module.

Incident irradiance on the PV panels under partial shading is not identical. The shaded PV modules affect the performance of the PV array by reducing the power throughput of the modules connected in series with it, thereby, reducing the maximum power of the PV array. The energy yield from the CI PV plant is reduced during partial shading. The reduction in energy yield due to partial shading depends on the shaded panels and the number of independent MPPT (also referred as MPPT granularity), which in case of CI is one. Further, the connection to the MV-AC grid requires a step-up transformer. The cost and volume occupied by the step-up transformer increases as the power rating of the PV plant increases. The transformer reduces the overall efficiency of the PV plant and results in decreased energy yield.

The need for the scalable PV plant and its control are discussed in [2], and large scale PV plant for urban area and their challenges are discussed in [3]. The family of Modular Multilevel Converters (MMC) is reliable, scalable and provides inherent modularity. The converter is built using basic power electronics blocks referred as sub-modules. The internal structure of the sub-module in the MMC has floating capacitors that forms floating DC-links. The use of MMC for utility scale PV plant has been recently proposed in [3]–[5]. MMC offers different possibilities for connection of the PV array to grid. Two important configurations are: (i) direct connection of the PV array to the DC link (or floating capacitors) of individual sub-module (referred as single stage inverter); (ii) connection of the PV array to the DC-link (or floating capacitors) using a DC-DC converter (referred as two stage inverter). When the classical inverter is replaced with the MMC the output harmonics are reduced due to increase in number of levels in the output voltage. However, the MPPT granularity is not increased if the PV array is connected to the DC link of the MMC. Therefore, the problem associated with partial shading is not addressed. The PV array when directly connected to the floating capacitors exploits the inherent modularity of the MMC and increases the MPPT granularity of the converter. Furthermore, by isolating the PV arrays and the floating capacitor using isolated DC-DC converters the MMC can be designed for direct connection to MV grid. The isolation is provided by a DC-DC converter which decouples the MPPT control from the MMC control and removes need for the step-up transformer at the Point of Common Coupling (PCC) [6]. However, the use of transformer at PCC is left to the discretion of Transmission System Operator (TSO). If the TSO insists on need of isolation at PCC, then the direct connection to MV grid with MMC results in isolation transformers, one at PCC and others interfacing PV and sub-modules. The absence of step-up transformer introduces additional requirement of limiting fault current on the MMC. The arm inductors have to be dimensioned properly to limit the current fed into PCC during the line faults. This will result in bulky arm inductors that has to be accounted for in the control to avoid impact on dynamic response.

The trend of utility PV plant is clearly to move towards more

This article has been accepted for publication in a future issue of this journal, but has not been fully edited. Content may change prior to final publication. Citation information: DOI 10.1109/TEC.2019.2930819, IEEE Transactions on Energy Conversion

distributed architecture, such as the MMC. The study in [7] shows that the addition of energy storage in PV plants reduces the LCOE considering the lifetime operation and discount rate. The MMC is a suitable topology for easily upgrading the PV plant with energy storage or to scale the PV plant to higher power levels. Although the MMC appears as a good solution for PV application, there are no studies comparing performance of the MMC for utility scale PV plant directly integrated into MV grid with the current state-of-the-art PV plants. Despite all the technical merits of the MMC, it is not clear whether the annual energy yield of such an inverter is higher than other distributed architecture of the utility scale PV plant. Further, higher initial cost of investment for the MMC based PV plant needs to be justified in terms of lower LCOE.

In this paper, the performances of two widely used utility scale PV plant arrangements are compared with MMC based PV plant directly connected to MV grid without step-up transformer. The figure of merits for comparison are efficiency, annual energy yield and cost of energy. An evaluation model of utility scale PV plant is proposed to compare the efficiency and annual energy yield. The efficiency of the power electronic converters are modeled based on the data obtained from the manufacturers. Since the MMC for direct integration into MV grid is in early stages of investigation, there is no specific converter topology of MMC available commercially for PV applications. The efficiency of the MMC is obtained through simulation using PLECS. In order to evaluate the performance of the MMC structure in realistic conditions, measured irradiance profiles for a one-year period at two different climates (India and Denmark) have been used.

A 3MW grid-connected CI based PV power plant at Kolar, Karnataka is chosen for the case study [8]. Another state-of-the-art PV plant configuration, Multi-String Central Inverter (MSCI), is considered for the analysis. A 3MW PV plant configuration using the MMC and the MSCI are designed with identical MPPT granularity. The efficiencies of the three PV plant configuration (CI, MSCI and MMC) and the annual energy yield considering identical irradiance profiles for a year is computed using a simulation model. The LCOE is calculated assuming 25 years as the operation life of the PV plant.

Section II describes the PV plant configurations and the inverter structures chosen for the MV grid. Section III gives a brief description on the design of MMC for direct MV grid integration and section IV presents the performance evaluation models chosen for this study. The performance assessment in terms of efficiency, annual energy loss and LCOE of the CI, MSCI and MMC is presented in section V. Finally, section VI describes the outcome of the study.

II. Configuration of PV Plant

A. Classic Converter Distribution of PV plant

The utility scale PV plants using single stage or two-stage converter arrangements, with 2L or 3L inverter, are referred to as classical structure. A line side step-up transformer facilitates the connection from LV grid to MV grid. The power transformer results in high volume, high cost and increased power losses. Fig. 1 shows the classical arrangements of PV plant connected to MV utility grid using step up transformer.

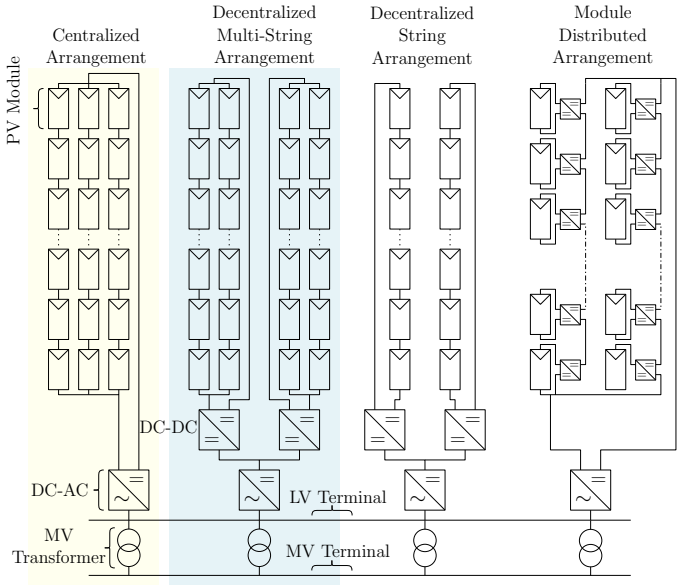

Fig. 1: Classical arrangement of the utility scale PV plant connected to MV grid, (a) Central Inverter (CI) arrangement, (b) Decentralized Multi-String Central Inverter (MSCI) arrangement, (c) Decentralized string arrangement and (d) Module distributed arrangement. The CI and MSCI configurations (highlighted in yellow and blue) are chosen for the study.

For utility scale PV plant, the configurations shown in Fig. 1(a) and (b) result in lower number of power electronic converters compared to configurations shown in Fig. 1(c) and (d). The configuration shown in Fig. 1(a) (referred as CI) and Fig. 1(b) (referred as MSCI) are considered for study which results in higher efficiency compared to other two configurations [1].

B. Modular Multilevel Converters in Utility Scale PV Power Plants

The variants of MMC described in [4] have emerged as alternate topologies compared to the classical inverters in PV plants. The topology provides inherent modularity, scalability and higher reliability compared to classical converters. The modularity of the MMC allows realization of a decentralized PV plant, therefore, it increases the MPPT granularity. The MMC is designed such that it facilitates the direct connection to the MV grid [6]. This avoids the need for the bulky line-side step-up transformer. As per the IEEE guidelines in [9], [10] the isolation between the renewable source and the utility grid need not necessarily be at the PCC. Therefore, the isolation is provided between the PV array and the MMC converter to avoid damages to the PV panels in case of MV applications as the PV panels have an isolation rating of 1000V. The newer PV panels are available with 1500V DC isolation; however, the isolation is still not at MV level. The required isolation is provided by using an isolated DC-DC converter between the PV array and the MMC.

Fig. 2 (a) shows the double star topology of the MMC. Each phase of the MMC has two arms and each arm is series connection of many individual sub-modules. Fig. 2 (b) shows the sub-module with a chopper cell topology and Fig. 2

This article has been accepted for publication in a future issue of this journal, but has not been fully edited. Content may change prior to final publication. Citation information: DOI 10.1109/TEC.2019.2930819, IEEE Transactions on Energy Conversion

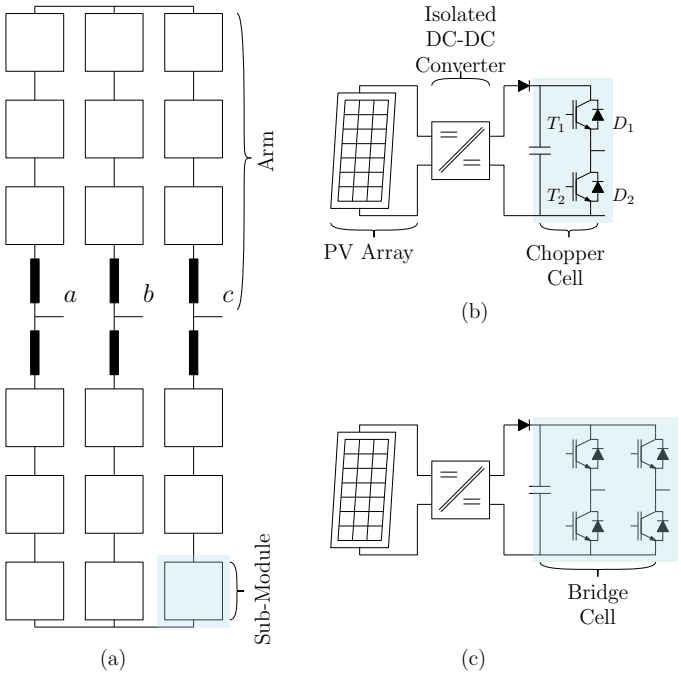

Fig. 2: (a) The Double Star MMC converter (b) The Chopper cell (Half-Bridge) realization of the Sub-Module with isolated DC-DC converter and PV array (b) Bridge cell (Full-Bridge) realization of the Sub-Module with isolated DC-DC converter and PV array.

(c) shows the SM with a bridge cell topology. The double star MMC with chopper cell based sub-module is referred as DSCC and the MMC with bridge cell based sub-module is referred as DSBC. Compared to all the MMC topology, the DSCC arrangement results in highest MPPT granularity with minimum number of switching devices. Compared to DSBC the DSCC has half the number of switches for the same number of MPPT granularity and compared to other MMC variants, such as star and delta topology, the MPPT granularity is doubled for same number of switching devices. However, in terms of efficiency the star and delta topology of the MMC and the DSCC-MMC have comparable efficiency [11] and scalability for direct connection to the MV grid.

C. PV Plant Chosen for Study

The DSCC-MMC in Fig. 2(a) with the sub-module using isolated dual active bridge DC-DC converters [12] as shown in Fig. 2(b), referred to as MMC here after, is chosen for this study. Two classical PV plant arrangements shown Fig. 1(a) Central Inverter (CI), and Fig. 1(b) Multi-String Central Inverter (MSCI) are considered for performance evaluation compared to the MMC topology. A 3MW grid-connected solar photovoltaic power plant at Kolar, Karnataka, India is considered for this case study [8]. The PV plant is divided into three 1MW segments. Each segment has four 250kW inverters connected to a 1MW step-up transformer. The MMC and MSCI configurations are designed with identical power rating as that of the CI configuration. The MSCI topology is designed to have the same modularity as the MMC topology resulting in identical MPPT granularity. The details of the CI PV plant are outlined in Table I.

TABLE I: PV Plant technical data [16]

Parameters	Symbols	Value
Medium Voltage (Nominal)	$V_{g(MV)}$	11kV
Low Voltage (Nominal)	$V_{g(LV)}$	230V
Apparent Power (Nominal)	S_N	3MVA
Grid Frequency	f_g	50Hz
Central Inverter Capacity	S_{CI}	250kVA
No. of Central Inverters	N_{CI}	12
MV Transformer Apparent Power	S_T	1.25MVA
PV Panel Maximum Power (Titan S6-60 series, Mono-crystalline)	P_{mp}	235Wp

III. Description of the Evaluation Model

The performance model for the PV plant is setup as shown in Fig. 3. The three PV plants, discussed in section II, are considered for evaluation. In case of MSCI and CI, the performance model of the central inverter is identical. The only difference is the additional DC-DC converter efficiency model for MSCI arrangement. The performance model is built in Simulink®. The five parameter model [13] of the PV panel is used to estimate the maximum power and the maximum operating voltage for a given effective irradiance and cell temperature. The advantage of using the five parameter model is that it requires only the manufacturer datasheet parameters to calculate the required coefficients as compared to King's model [14] that needs additional experimental data to calculate the model coefficients. The PV array output fed to the MSCI and MMC configurations is identical. The PV cell temperature is estimated as per [14] based on the ambient temperature data. The efficiency curves of the converters are used in the model, avoiding the errors due to parameterization. The model for performance evaluation of the PV array, converters are discussed in this section. The transformer performance model proposed in [15] is used for the analysis.

A. PV Array Performance Model

The energy yield of the power plants are compared against the same set of effective irradiance and module temperature. To have a good data accuracy from the two PV array configurations and to reduce the output error from PV performance model, the maximum power and the voltage at maximum power available from the PV module (Titan S6-60-2-235) are obtained using the five parameter model [13] and parameterized as a second order polynomial using MathWorks curve fitting toolbox [16] with an error less than 0.5%, expressed in (1), as a function of irradiance (G) and temperature (T) ,

$$f(G,T) = a_0 + a_1 G + a_2 G^2 + a_3 T + a_4 T^2 + a_5 GT \quad (1)$$

The coefficients of the polynomial in (1) are tabulated in Table. II. The look-up table for maximum power operating points of the PV module can be reconstructed using (1). The PV array is obtained by connecting the required number of PV modules in series and parallel.

The net maximum power of the PV array (P_{amp}) and the voltage at the maximum power (V_{amp}) are the output

This article has been accepted for publication in a future issue of this journal, but has not been fully edited. Content may change prior to final publication. Citation information: DOI 10.1109/TEC.2019.2930819, IEEE Transactions on Energy Conversion

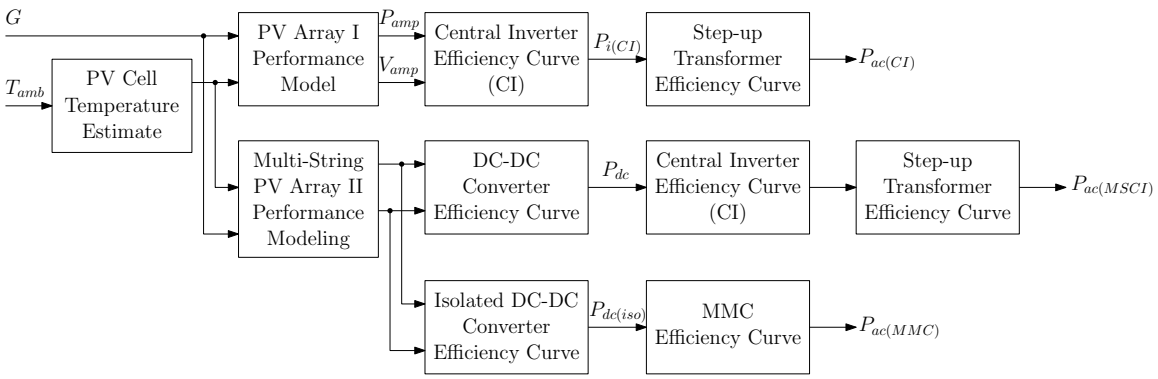

Fig. 3: Block diagram representation of performance model to obtain the power of the PV plant as a function of irradiance and PV cell temperature.

TABLE II: Coefficients of the polynomial in (1) for P_{mp} and V_{mp}, respectively.

$f(G,T)$	a_0	a_1	a_2	a_3	a_4	a_5
P_{MP}	98.08	56.27	-0.9347	-12.91	-0.0142	-7.256
V_{MP}	24.66	0.3922	-0.4573	-3.142	0.0232	0.0960

from the performance model. The output for two PV array configuration are accurately obtained using (2). The number of PV modules in series is represented by N_s and in parallel by N_p, respectively.

$$P_{amp} = \sum_{j=1}^{N_p} \sum_{i=1}^{N_s} P_{mp_{ij}}(G_{ij}, T_{ij})$$
$$V_{amp} = \sum_{i=1}^{N_s} V_{mp_{ij}}(G_{ij}, T_{ij}) \quad (2)$$

The PV modules in series is $N_s = 24$ and in parallel is $N_p = 45$ for the PV array configuration used in CI and for the PV array configuration used for MSCI and MMC $N_s = 27$ and $N_p = 1$.

B. Performance Model of Inverters and DC-DC Converters

The optimized design procedure of the MMC, suggested in [6] for direct connection of the MMC to the MV grid, is employed to calculate the MMC parameters. A balanced three phase MMC is considered, the system is designed for the data shown in Table I. The value of the parameters are shown in Table III. Analytical expression for inverter performance model is discussed in [17]. The model must account for the inverter efficiency at MPP voltages and the efficiency of MPPT algorithm. In order to obtain accurate results and minimize the model-induced errors, the maximum efficiency is obtained from the datasheet. The inverter and MPPT efficiencies are modeled using two dimensional look-up tables. The classical PV plant chosen for this analysis has 12 identical central inverters, each rated for 250kW. The central inverter from Advance Energy Industries (AE 250NX) [18] that has the highest CEC efficiency among other commercially available inverters for rated power is chosen for this study, the maximum efficiency is 98% and CEC efficiency is 97.5%, as per [19].

TABLE III: Parameters of MMC Converters

Parameters	**Symbol**	**Value**
Rated Apparent Power	S_R	3MVA
Rated Voltage (l-n)	V_R	11kV
Rated Output Current	I_R	91A
Nominal Frequency	f_s	50Hz
DC Link Voltage	V_{dc}	36kV
Sub-Module Capacitance	C	1mF (0.0263pu)
Arm Inductance	L_a	12mH (0.0312pu)
SM Voltage	V_{SM}	900V
Maximum SM Voltage	$V_{SM(max)}$	1020V
Switching Frequency	f_{sw}	333Hz
SM Rated Power	P_{SM}	12.5kW

Fig. 4 shows the inverter efficiency as a function of the DC link voltage and the operating power.

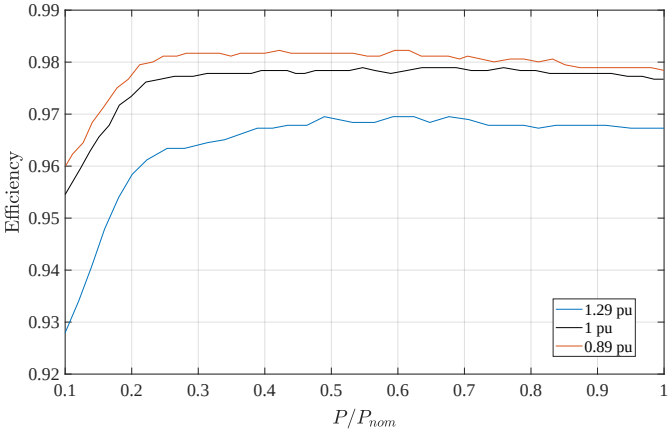

Fig. 4: The inverter CEC efficiency curve for Advance Energy Industries AE 250NX (98% maximum value) as a function of operating power and DC link voltage (1pu=740V) [19].

The MMC as a PV inverter operates at fixed sub-module capacitor voltages, therefore, avoiding the variation of efficiency as seen in CI due to DC link voltage variation. The power losses of the MMC module are calculated using PLECS simulation software. The sub-module chopper cell uses the Infineon dual IGBT modules (FF150R17KE4) as switching device with voltage rated at 1700V (nominal operating voltage

This article has been accepted for publication in a future issue of this journal, but has not been fully edited. Content may change prior to final publication. Citation information: DOI 10.1109/TEC.2019.2930819, IEEE Transactions on Energy Conversion

of 900V) and 150A nominal current. In order to obtain the worst-case energy yield for the MMC, the full load power losses due to the arm inductors and submodule capacitors are retained for the entire operating range. Fig. 5 shows the MMC output voltages, output currents, three phase output power and upper arm currents for a duration of 50ms. The MMC delivers 3MW power to the load and maintains balanced operation. Each phase of the MMC carries equal fraction of DC current as seen from the arm currents. Fig. 6 shows the insertion indexes and the inserted arm voltage, the ripple current due to staircase waveform is filtered by the arm inductor. Fig. 7 shows the IGBT (T_1, T_2) and body diode (D_1,D_2) currents for a sub-module. The choice of PWM strategy and switching frequency has an impact on the MMC efficiency [20]. The converter is, therefore, controlled using the open-loop control with nearest level switching [21]. This switching strategy yields lower switching loss as the sub-modules are switched at low frequency. The PLECS IGBT model allows to feed in the turn-on and turn-off energy data at various magnitudes of the device current and temperatures along with the V-I characteristics and the thermal impedance.

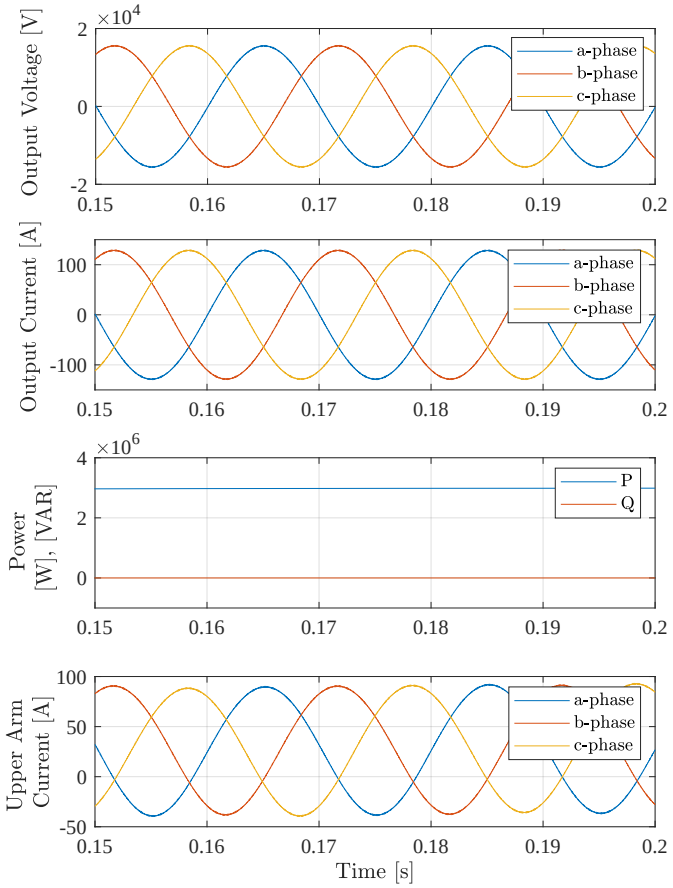

Fig. 5: The three phase output voltage, current, power and upper arm currents of the MMC.

The block diagram of the MMC switching model and loss calculation is shown in Fig. 8. The maximum allowed junction temperature is set to 120°C. The thermal impedance of the case to heatsink is chosen to be 0.01K/W so that the device

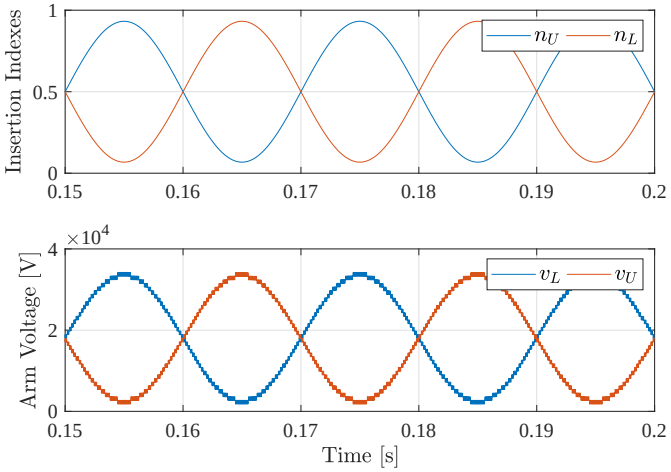

Fig. 6: The insertion indexes (n_U, n_L) and the inserted arm voltages (v_U, v_L) for phase 'a' upper (U) and lower (L) arms of the MMC.

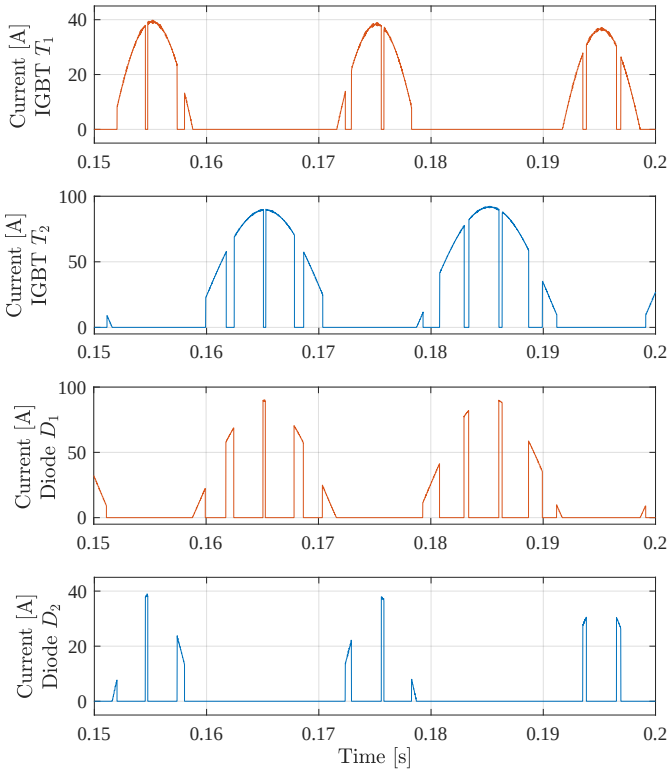

Fig. 7: PLECS model to obtain power loss in the MMC as a function of junction temperature and electrical load.

junction temperature is close to the limit as seen in Fig. 9. In PLECS the junction temperature dependent switching and conduction losses are obtained. Fig. 10 shows the efficiency of the MMC at 900V on each of the sub-module capacitor at different operating power. To assess the performance of the MMC, the efficiency profile is decreased in steps of 1% so that the lowest possible efficiency profile of the MMC has maximum efficiency of 94.4%. The best and worst case efficiency profile will account for the decrease in efficiency that can occur due to unbalance within the MMC as a result of asymmetric power generation owing to unequal irradiance and

This article has been accepted for publication in a future issue of this journal, but has not been fully edited. Content may change prior to final publication. Citation information: DOI 10.1109/TEC.2019.2930819, IEEE Transactions on Energy Conversion

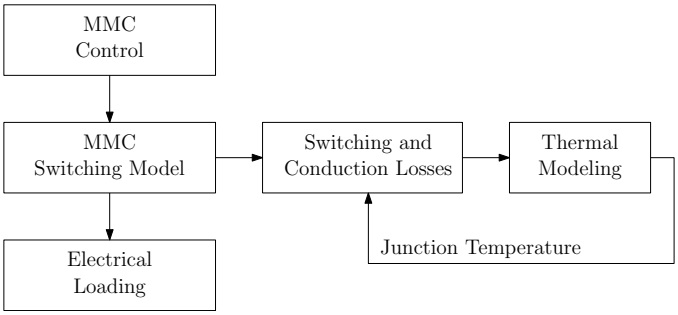

Fig. 8: PLECS model to obtain power loss in the MMC as a function of junction temperature and electrical load.

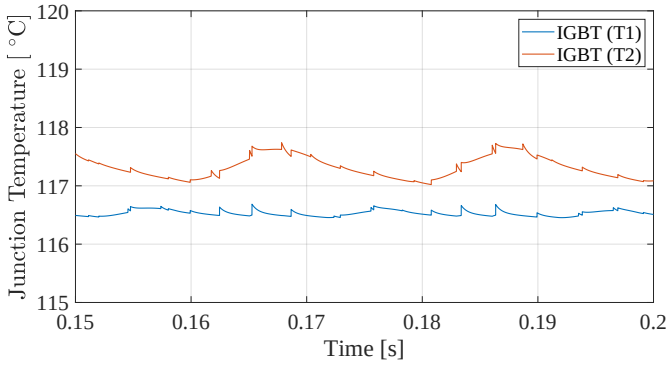

Fig. 9: The junction temperature of the IGBTs in the sub-module of the MMC under full operating load.

increased MPPT granularity. The main advantage of the MV DC-link of the MMC is the direct connection to the MV grid. This reduces the magnitude of current carried by the phases of the MMC. Each arm of the MMC carries half the rated output current, which further reduces the conduction losses in the MMC. Due to low switching frequency of the sub-modules and the reduced nominal current in arm of the MMC, the switching and conduction losses are reduced significantly.

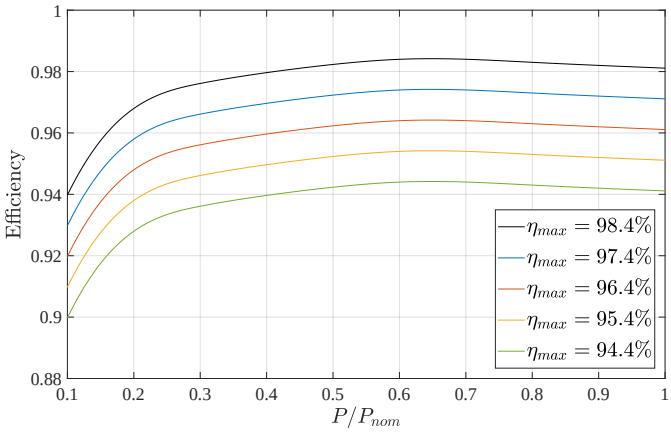

Fig. 10: Efficiency curves of the MMC including the losses in the filters. The efficiency curves are obtained using MMC model in PLECS. Infineon dual IGBT modules ,FF150R17KE4, is used as switching device per sub-module. The profile of the efficiency curve is retained and the efficiency is effectively decreased in steps of 1% from $\eta_{max} = 98.4\%$ to $\eta_{max} = 94.4\%$.

The MMC inverter uses additional high power isolated DC-DC converters. The voltage rating of the sub-module is matched with the commercially available DC-DC converter nominal voltage. For power level in tens of kilo-watts the dual active isolated bridge converters are preferred, the efficiency of such SiC MOSFET based converters are in the range of 97%-98% [12]. The additional power loss is around 1% when Si-IGBT is considered for switching in place of SiC MOSFET. Fig. 11 shows the efficiency curve of the DC-DC isolated dual active converter. In case of the MSCI PV plant, the same number of DC-DC converters are used as in the MMC to obtain a fair comparison. The DC-DC converter in this case does not have an isolation transformer. The maximum efficiency of such DC-DC converter excluding the isolation transformer is in the range of 99% even at low partial loads [22], [23]. Fig. 12 shows the efficiency curves of the DC-DC converter. Typically, the PV multi-string optimizer (DC-DC) has efficiency in the range of 99% to 99.5%.

IV. Comparative Assessment of Classical and MMC PV Plant

The irradiance, temperature and wind speed can be modeled as a stochastic process that is influenced by time of day,

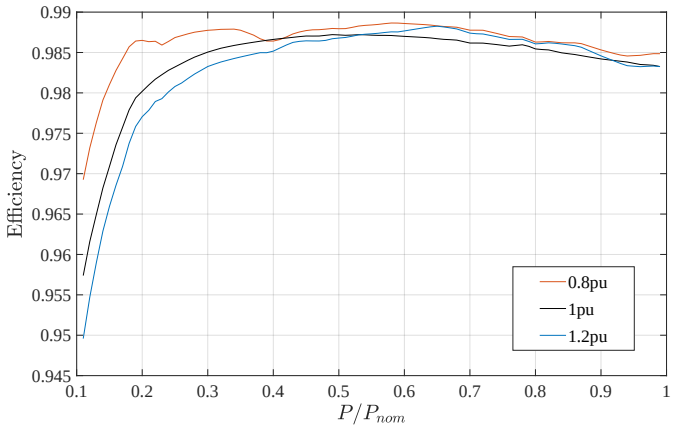

Fig. 11: Efficiency of the IGBT based dual active isolated bridge converter switching at 10kHz [12] for different DC link voltage (1pu=750V).

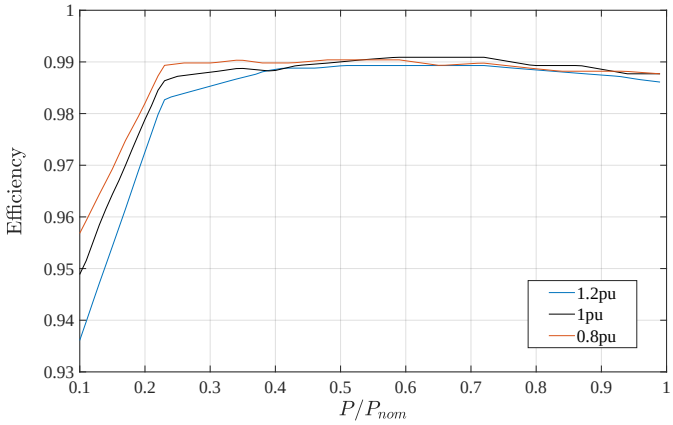

Fig. 12: Efficiency of the IGBT based DC-DC converter at different DC link voltage [22], [23] (1pu=750V).

This article has been accepted for publication in a future issue of this journal, but has not been fully edited. Content may change prior to final publication. Citation information: DOI 10.1109/TEC.2019.2930819, IEEE Transactions on Energy Conversion

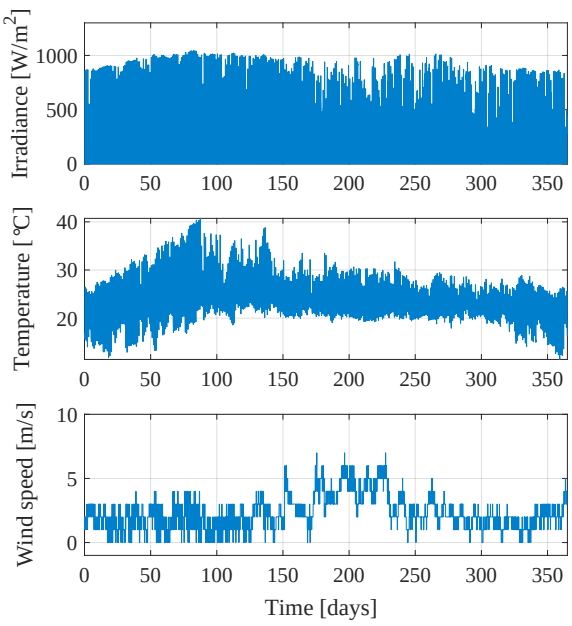

Fig. 13: The irradiance, temperature and wind speed monitored between January 2014 to December 2014 with 60min average [24], measured at Bangalore, India (station ID 35059).

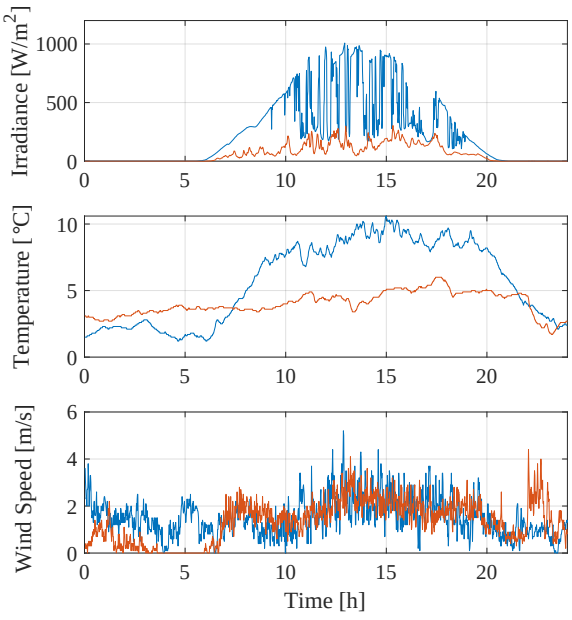

Fig. 14: Irradiance, temperature and wind speed profile measured at Aalborg, Denmark [25]. The first profile (blue) is with relatively high irradiance and the second profile (red) is for low irradiance.

geographic location and season. The data obtained over a year from January [24] for the plant location is used for evaluating the annual energy production, as shown in Fig. 13. Two different irradiance profiles, low and high, measured at Aalborg (Denmark) with sample time of 1 minute are considered for evaluating efficiency [25] as shown in Fig. 14. The temperature and wind speed are measured with the same sampling time.

TABLE IV: Annual energy obtained from three different configuration of PV plant.

PV Plant	**Maximum Annual Energy** (MWh)	**Annual Energy Extracted** (MWh)
CI	5796	5205
MSCI		5218
MMC ($\eta_{max} = 98.4\%$)		5515
MMC ($\eta_{max} = 94.4\%$)		5290

A. Annual Energy Yield and Efficiency

The annual energy obtained by the PV plants is tabulated in Table IV for all three PV plant configurations. The annual energy obtained by the MMC PV plant for two different efficiency curves is compared with CI and MSCI PV plants. It is seen that the annual energy extracted from the MMC PV plant for the lowest and highest efficiency profile is 1.63% and 5.95% higher than the one extracted from the CI PV plant, respectively. The MMC PV plant provides higher annual energy yield compared to CI. In case of MSCI PV plant, annual energy generation is 0.2% higher compared to CI PV plant. This a marginal improvement in terms of annual energy compared to CI PV plant.

The annual energy losses in each of the PV plant for a given converter structure is shown in Fig. 15. The annual energy loss which is the difference of total energy yield between a 100% efficient PV plant and the three different configurations (CI, MSCI and MMC). Annual energy loss due to individual units in the PV power plant are calculated as integral of power loss over a year between the stages in Fig. 3 for CI, MSCI and MMC using (3). Where P_{in} is power input to each stage and P_{out} is power out of each stage in the performance model. The percentage value is obtained by dividing the annual energy loss of each unit with maximum annual energy. The maximum annual energy is integral of output power from the PV array, P_{amp}, over a span of one year.

$$Energy\ Loss = \int_0^T (P_{in} - P_{out})\, dt \tag{3}$$

The annual energy losses due to MPPT algorithm are greater than a factor of two for centralized PV plant compared to MMC or MSCI. However, this is highly dependent on the plant layout conditions, location and surroundings. The suggested annual energy loss due to MPPT are typical in PV plant with retrofit where the old and new PV panels are mixed. In the case of CI, the variation in the voltage due to MPPT algorithm is across entire PV array resulting in higher power loss compared to other configurations. The main advantage of the MMC is evident due to lower energy losses at inverter stage. The annual energy losses for MSCI PV plant, ignoring the energy losses due to the transformer, is comparable to the MMC at low efficiency ($\eta_{max} = 94.4\%$). The net efficiency obtained as ratio of the power at the MV terminal to the maximum power generated by the PV array at particular irradiance level

This article has been accepted for publication in a future issue of this journal, but has not been fully edited. Content may change prior to final publication. Citation information: DOI 10.1109/TEC.2019.2930819, IEEE Transactions on Energy Conversion

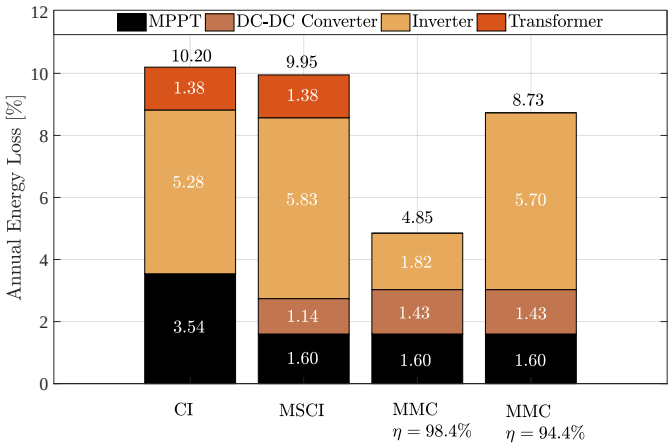

Fig. 15: Annual energy loss (compared to maximum annual energy, refer to Table IV) at different stages of the PV plant.

TABLE V: Energy Efficiency of the PV plants for two different irradiance profiles.

Effective Efficiency of the PV Plant		
PV Plant	**High Irradiance Profile**	**Low Irradiance Profile**
CI	88.89%	86.18%
MSCI	89.80%	86.92%
MMC ($\eta_{max} = 99\%$)	95.66%	93.80%
MMC ($\eta_{max} = 95\%$)	91.85%	90.06%

is shown in Fig. 16. The net efficiency is expressed in (4), where i=CI, MSCI, MMC respectively.

$$\eta_{net} = \left.\frac{P_{ac(i)}}{P_{amp}}\right|_G \tag{4}$$

For PV plant based on CI the net efficiency is product of central inverter efficiency and transformer efficiency. In case of the MSCI and the MMC the additional DC-DC converter efficiency is accounted. It is seen that the MMC PV plant has a maximum net efficiency of 95.2% and 91.6% for two different efficiency curves of MMC ($\eta_{max} = 98.4\%$ and $\eta_{max} = 94.4\%$) between irradiance of $300 - 1000W/m^2$. The CI has a linear efficiency curve with efficiency varying between 86% to 91.5%. The MSCI has an average efficiency of 90% between irradiance 300 to $1000W/m^2$. From the efficiency curves, it is seen that the net efficiency of the MMC is higher than the CI and MSCI in both low and high irradiance. In case of MSCI, the efficiency is higher than CI between irradiance $175 - 750W/m^2$. For the location considered (Kolar, Karnataka, India) the average variation in irradiance is between $600 - 1000W/m^2$. Therefore, the annual energy of the CI and MSCI are comparable. For regions where the average variation in the irradiation is between 200 to 700W/m2 (such as Aalborg, Denmark) the MSCI PV plant will have a better yield compared to CI PV plant. The efficiency for low and high irradiance profiles is shown in Table. V.

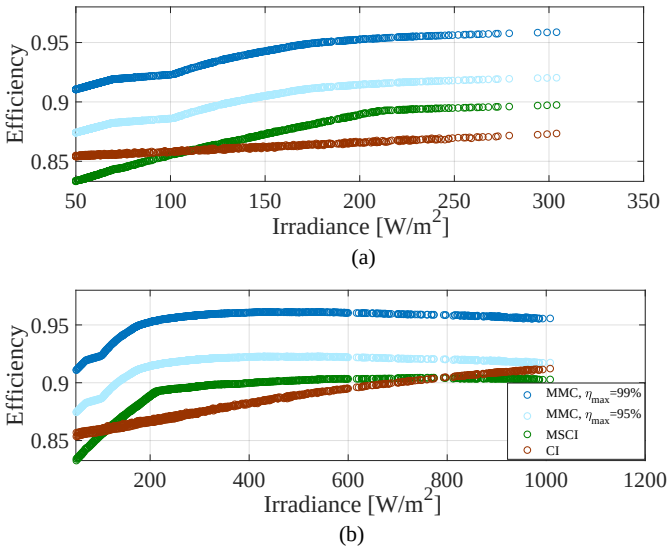

Fig. 16: Efficiencies of the PV Plants (a) at low irradiance profile with low temperature (b) at high irradiance profile with high temperature.

TABLE VI: Converter and transformer/filter costs for all the three PV plant configurations (cost in Euro).

Converter Cost	**CI**	**MSCI**	**MMC**
Inverter	154584	154584	—
DC/DC Converter	—	109440	277200
Sub-Module	—	—	45840
Transformer and Filter Cost			
Transformer	53178	53178	—
Filter	1418	1418	620
Total Cost	209180	318620	323660

B. Levelized Cost of Energy

In order to properly compare all the configurations, the LCOE is evaluated in this section [26], [27]. It takes into account both the extracted energy over the lifetime of the plant and the life cycle cost of the studied structures:

$$LCOE = \frac{Total\ life\ cycle\ cost}{Energy\ produced\ over\ lifetime}\left(\frac{EUR}{MWh}\right) \tag{5}$$

The lifetime cost of all the three PV plant configurations is firstly evaluated. It can be mainly divided in four parts: PV cost, converter cost, transformer/filter cost and fixed cost. The nominal power of the system is 3 MVA; the total cost for the PV arrays is €6000000 and the fixed cost is €950228 [8] have been taken into consideration in this work. The converter cost and the transformer/filter cost depend on which PV plant configuration is chosen. Table VI depicts these costs for all the considered configurations. The inverter cost for all the configurations are evaluated.

The CI configuration consists of 12 inverters. The cost of each inverter (assuming 2-L) has been evaluated to €12882. For CI, the IGBT cost is approximately €1600 and DC link capacitor cost is €3300. Then the total cost for all the inverters is €154584. In addition, three transformers and a

This article has been accepted for publication in a future issue of this journal, but has not been fully edited. Content may change prior to final publication. Citation information: DOI 10.1109/TEC.2019.2930819, IEEE Transactions on Energy Conversion

TABLE VII: Extracted energy, total cost and LCOE for all the configurations in per unit.

	Extracted Energy (p.u.)	**Total Cost (p.u.)**	**LCOE (p.u.)**
CI	1.000	1.000	1.000
MSCI	1.002	1.015	1.013
MMC	1.059	1.016	0.959

filter have been considered with a cost of €17726 and €1418, respectively [28]. The multi-string central inverter (MSCI) has the same costs of the centralized inverter (CI) plus the additional DC/DC converters per PV strings. In this work 240 DC/DC converter are considered. Each converter needs four 1700V/120A IGBT (€89 each) and an output filter (€100 each). Finally, the MMC cost is evaluated. In this case no inverter is taken into account but the DC/DC isolated converter cost and the sub-module cost have to be calculated. The DC/DC isolated converter uses eight 1700V/120A IGBT (€89 each) plus a transformer that costs about €443. The sub-module consists of two 1700V/120A IGBT and a capacitor of 1mF with a cost of €13. Having the isolation in the DC/DC converter and the ability of the MMC for direct connection to the MV grid, the main transformer can be avoided and only the filter is used. Its cost is €620 [28]. Once having evaluated the life cycle cost and the extracted energy (in the previous section), the LCOE can be calculated. Table VII shows the LCOE for all the structures in per unit (p.u.) considering the LCOE of the centralized inverter as the base unit quantity (€7186000). It also shows the total cost and the total extracted energy in p.u.

From Table VII, it is easy to note that the 1.6% higher cost of the MMC is compensated by an increase of 5.95% of extracted energy in comparison with the central inverter configuration. Moreover, the MMC presents a lower LCOE in comparison with the other configurations. By considering an energy price equal to 0.1 /kWh, the payback period for the MMC is 13.1 years. For the other two configurations, CI and MSCI, it is 13.8 years and 14.0 years respectively.

V. Conclusion

The arrangement of the PV plant using central inverter, the decentralized arrangement with multi-string central inverter and the modular multilevel converter have been analyzed in terms of the energy yield, LCOE and efficiency for PV plant for medium voltage applications. The MMC annual energy losses for two different efficiency curves with peak value of 98.4% and 94.4%, has been evaluated. Annual energy loss for the MMC PV plant with peak efficiency of $\eta = 98.4\%$ is 52.45% lower compared to the central inverter PV plant and 14.4% lower with peak efficiency of $\eta = 94.4\%$. The MMC topology, as well as the multi-string central inverter, has lower MPPT losses due to the distributed MPPT in comparison with the central inverter.

The lower power losses due to the MMC and the absence of energy losses due to the transformer justify the use of isolated DC-DC converter to provide the necessary isolation for protection of PV module. Since the distribution system operators may require a transformer at the PCC, the analysis shows that better annual energy yield is achieved with transformer at PCC as well as isolation transformer at DC-DC converter in comparison with the central inverter and the multi-string central inverter. Moreover, in case of the MMC PV plant, if the transformer is used for isolation at PCC, the voltage need not be stepped up. Therefore, the cost and the power losses of the transformer are reduced.

The cost of the MMC is higher compared to central inverter and multi-string central inverter, however, the LCOE of the MMC is 4.1% lower than the central inverter and the multi-string central inverter, respectively. The DSCC-MMC, therefore, is a viable alternative converter topology for direct integration of PV plant to MV grid with lower LCOE compared to classical central inverter used in PV plants.

References

[1] A. Cabrera-Tobar, E. Bullich-Massagué, M. Aragüés-Peñalba, and O. Gomis-Bellmunt, "Topologies for large scale photovoltaic power plants," *Renewable and Sustainable Energy Reviews*, vol. 59, pp. 309–319, Jun. 2016.

[2] Y. Xue, K. C. Divya, G. Griepentrog, M. Liviu, S. Suresh, and M. Manjrekar, "Towards next generation photovoltaic inverters," in *2011 IEEE Energy Conversion Congress and Exposition*, Sep. 2011, pp. 2467–2474.

[3] S. Rivera, B. Wu, R. Lizana, S. Kouro, M. Perez, and J. Rodriguez, "Modular multilevel converter for large-scale multistring photovoltaic energy conversion system," in *2013 IEEE Energy Conversion Congress and Exposition*, Sep. 2013, pp. 1941–1946.

[4] H. Akagi, "Classification, Terminology, and Application of the Modular Multilevel Cascade Converter (MMCC)," *IEEE Transactions on Power Electronics*, vol. 26, no. 11, pp. 3119–3130, Nov. 2011.

[5] M. R. Islam, Y. Guo, and J. Zhu, "Multiple-input multiple-output medium frequency-link based medium voltage inverter for direct grid connection of photovoltaic arrays," in *2013 International Conference on Electrical Machines and Systems (ICEMS)*, Oct. 2013, pp. 202–207.

[6] A. Hillers and J. Biela, "Optimal design of the modular multilevel converter for an energy storage system based on split batteries," in *2013 15th European Conference on Power Electronics and Applications (EPE)*, Sep. 2013, pp. 1–11.

[7] G. Tsolaridis, H. A. Pereira, A. F. Cupertino, R. Teodorescu, and M. Bongiorno, "Losses and cost comparison of DS-HB and SD-FB MMC based large utility grade STATCOM," in *Environment and Electrical Engineering (EEEIC), 2016 IEEE 16th International Conference On*. IEEE, 2016, pp. 1–6.

[8] H. Mitavachan, A. Gokhale, and J. Srinivasan, "3-MW scale grid-connected solar photovoltaic power plant at Kolar, Karnataka."

[9] "IEEE Application Guide for IEEE Std 1547(TM), IEEE Standard for Interconnecting Distributed Resources with Electric Power Systems," *IEEE Std 1547.2-2008*, pp. 1–217, Apr. 2009.

[10] C. Schauder, "Impact of FERC 661-A and IEEE 1547 on Photovoltaic inverter design," in *2011 IEEE Power and Energy Society General Meeting*, Jul. 2011, pp. 1–6.

[11] A. Hillers, M. Stojadinovic, and J. Biela, "Systematic comparison of modular multilevel converter topologies for battery energy storage systems based on split batteries," in *2015 17th European Conference on Power Electronics and Applications (EPE'15 ECCE-Europe)*, Sep. 2015, pp. 1–9.

[12] H. Akagi, T. Yamagishi, N. M. L. Tan, S. i Kinouchi, Y. Miyazaki, and M. Koyama, "Power-loss breakdown of a 750-V, 100-kW, 20-kHz bidirectional isolated DC-DC converter using SiC-MOSFET/SBD dual modules," in *2014 International Power Electronics Conference (IPEC-Hiroshima 2014 - ECCE ASIA)*, May 2014, pp. 750–757.

[13] W. De Soto, S. A. Klein, and W. A. Beckman, "Improvement and validation of a model for photovoltaic array performance," *Solar Energy*, vol. 80, no. 1, pp. 78–88, Jan. 2006.

[14] D. L. King, J. A. Kratochvil, and W. E. Boyson, *Photovoltaic Array Performance Model*. United States. Department of Energy, 2004.

[15] K. N. D. Malamaki and C. S. Demoulias, "Analytical Calculation of the Electrical Energy Losses on Fixed-Mounted PV Plants," *IEEE Transactions on Sustainable Energy*, vol. 5, no. 4, pp. 1080–1089, Oct. 2014.

[16] *Curve Fitting Toolbox™User's Guide*, 2017. [Online]. Available: www.mathworks.com
[17] D. L. King, S. Gonzalez, G. M. Galbraith, and W. E. Boyson, "Performance model for grid-connected photovoltaic inverters," *Sandia National Laboratories, Tech. Rep*, 2007.
[18] "AE 250NX — Commercial Solar Inverters — AE Solar Energy," http://solarenergy.advanced-energy.com/commercial-solar-inverters/ae-250nx.
[19] "Inverters," http://www.gosolarcalifornia.ca.gov/equipment/inverters.php.
[20] A. Hassanpoor, S. Norrga, and A. Nami, "Loss evaluation for modular multilevel converters with different switching strategies," in *2015 9th International Conference on Power Electronics and ECCE Asia (ICPE-ECCE Asia)*, Jun. 2015, pp. 1558–1563.
[21] L. Angquist, A. Antonopoulos, D. Siemaszko, K. Ilves, M. Vasiladiotis, and H. Nee, "Open-Loop Control of Modular Multilevel Converters Using Estimation of Stored Energy," *IEEE Transactions on Industry Applications*, vol. 47, no. 6, pp. 2516–2524, Nov. 2011.
[22] "VP5000 - DC DC Converter," http://www.aradex.de/.
[23] "Possible use of DC/DC converters," https://www.aradex.de/en/system-solutions/whitepaper-power-electronics/possible-use-of-bidirectional-dcdc-converters/.
[24] "System Advisor Model (SAM) —," https://sam.nrel.gov/.
[25] "Photovoltaic Systems—," http://www.et.aau.dk/research-programmes/photovoltaic-systems/.
[26] M. Campbell, P. Aschenbrenner, J. Blunden, E. Smeloff, and S. Wright, "The drivers of the levelized cost of electricity for utility-scale photovoltaics," *White Paper: SunPower Corporation*, 2008.
[27] R. Knorr, "Design criteria and levelized costs of electricity for photovoltaic power plants at different global locations," in *International Multi-Conference on Systems, Sygnals Devices*, Mar. 2012, pp. 1–6.
[28] Y. Xue, B. Ge, and F. Z. Peng, "Reliability, efficiency, and cost comparisons of MW-scale photovoltaic inverters," in *2012 IEEE Energy Conversion Congress and Exposition (ECCE)*, Sep. 2012, pp. 1627–1634.